# Energetics of the Sequential Electroreduction and Electrooxidation Steps of Benzenoid Hydrocarbons[1)]

Tanekazu KUBOTA,* Kenji KANO, Bunji UNO, and Tomonori KONSE
Gifu Pharmaceutical Universtiy, 5-6-1 Mitahora-higashi, Gifu 502
(Received May 6, 1987)

The first and second reduction ($E^{red}_{1/2\cdot1}$, $E^{red}_{1/2\cdot2}$) and the first oxidation ($E^{oxd}_{1/2\cdot1}$) standard potentials of benzenoid alternant hydrocarbons (BAH) were experimentally determined by means of cyclic voltammetry (CV) in nonaqueous solvents. The second standard oxidation potential ($E^{oxd}_{1/2\cdot2}$) was, however, estimated by checking the scan rate dependence of the irreversible CV curve. The equations pertinent to these potentials and their mutual relations were formulated from the points of view of the Born–Haber-type thermodynamic energy cycle and SCFMO calculations. Of the SCFMO calculations, the MO-paring property established in the PPP-type π-electron theory was very successful in the discussion of the equations given above. Under the acceptable assumptions that the solvation energies due to mono- and dications are put equal to those of the mono- and dianions respectively, and using the MO-pairing property, the equation of $(E^{oxd}_{1/2\cdot1}+E^{red}_{1/2\cdot1})=(E^{oxd}_{1/2\cdot2}+E^{red}_{1/2\cdot2})$ was derived. The experimental results were well described by this equation. The solvation-energy values were evaluated by applying the experimentally determined reduction or oxidation potentials to the theoretical equations. An examination of the solvation energies has shown that these values can be interpreted by means of the Born-type equation.

It is well-known that the voltammetric reduction and oxidation of usual organic substances show two waves in nonaqueous solvents;[2–5)] these waves are correlated with the formation of the monoanion radical $R^-$ and the dianion $R^=$ for the reduction and the monocation radical $R^+$ and the dication $R^{++}$ for the oxidation. Especially, the voltammetric reduction and oxidation behavior of aromatic hydrocarbons in nonaqueous solvents has been studied by many workers in connection with their investigations of the radical ions themselves or electrochemical and chemical reactions immediately following the radical-ion formation.[6–8)] The molecular orbital description for the first half-wave reduction ($E^{red}_{1/2\cdot1}$) and oxidation ($E^{oxd}_{1/2\cdot1}$) potentials was also discussed[6–15)] and written by the sum of the LUMO ($\varepsilon_{lu}$) or HOMO ($\varepsilon_{ho}$) energy and the solvation energy, as is given by Eqs. 1 and 2:[7–15)]

$$FE^{red}_{1/2\cdot1}(R^-/R) = \Delta G^\circ - \varepsilon_{lu} - \Delta E^-_{solv} \quad (1)$$

$$FE^{oxd}_{1/2\cdot1}(R^+/R) = \Delta G^\circ - \varepsilon_{ho} + \Delta E^+_{solv} \quad (2)$$

where the absolute potential of a reference electrode is denoted by $\Delta G^\circ$[16)] and where $\Delta E^-_{solv}=(E^-_{solv}-E_{solv})$ and $\Delta E^+_{solv}=(E^+_{solv}-E_{solv})$ are the solvation-energy difference between monoanion and neutral species and that between monocation and neutral species respectively. The linear relation of the $E^{red}_{1/2\cdot1}$ vs. $\varepsilon_{lu}$ plot or the $E^{oxd}_{1/2\cdot1}$ vs. $\varepsilon_{ho}$ plot has been reported using HMO or semiempirical SCFMO;[6–15,17–19)] also, the values of $\Delta E^-_{solv}$ and $\Delta E^+_{solv}$ have been estimated by means of Eqs. 1 and 2.[12)] In turn, Hush and Blackledge[20)] discussed first the reduction potential difference between $E^{red}_{1/2\cdot1}$ and $E^{red}_{1/2\cdot2}$ (the second half-wave reduction potential) by using π-SCFMO in neutral species, showing that the difference stands for the free-energy change pertinent to the disproportionation $2R^- \rightleftarrows R+R^=$ and is in intimate correlation with the two-electron-repulsion-integral $\gamma_H$ at LUMO.[20,21)] However, the monoanion and dianion are necessarily in a quite different electronic structure from that of the neutral species, so that their discussion is only qualitative. Keeping this fact in mind, in a previous paper[19)] we ourselves again discussed and formulated the mutual relation between $E^{red}_{1/2\cdot1}$ and $E^{red}_{1/2\cdot2}$ from the points of view of the Born-Haber-type thermodynamic energy cycle and SCFMO calculation under the assumption that the above reduction waves are for a reversible system. The theoretical equations thus formulated were experimentally examined using stilbene derivatives as model substances, with the result that the theoretical and experimental outcomes were found to be reasonably compatible.[19)] Here we have newly derived the equations with regard to the mutual relation between the first ($E^{oxd}_{1/2\cdot1}$) and the second ($E^{oxd}_{1/2\cdot2}$) half-wave oxidation potentials. The equations mentioned above on the first and second reduction and oxidation potentials and their mutual correlations have been quantitatively examined using benzenoid alternant hydrocarbons (BAH) in order to verify their reliability, because the BAH's are the fundamental substances for testing a theoretical treatment. In addition, the solvation energies of the monoanion, monocation, dianion, and dication were evaluated using the above equations. The details of these examinations will be reported here.

## Experimental

**Cyclic Voltammetry.** The half-wave reduction potentials of various kinds of BAH were polarographically reported by Hoytink et al.[2,6)] and later by other workers in nonaqueous solvents.[7–12,22,23)] Hoytink's data were mainly obtained in 75 and 96 % aqueous dioxanes vs. a saturated calomel electrode (SCE).[2,6)] However, the data of $E^{red}_{1/2\cdot2}$ were not sufficient. Parker and his colleagues[8,15)] also carried out

much work on the nonaqueous voltammetries of BAH and other organic substances; they recommended the use of neutral alumina,[24] which is added in a nonaqueous sample solution in order to remove the moisture thoroughly from nonaqueous solvents so that one can record the reversible cyclic voltammograms (CV) for $E^{red}_{1/2\cdot2}$ as well as the $E^{red}_{1/2\cdot1}$ and $E^{oxd}_{1/2\cdot1}$, and also for $E^{oxd}_{1/2\cdot2}$ in some organic substances. For our present purpose, the measurement of reduction and oxidation potentials in reversible redox systems of BAH is, of course, to be hoped for, so much effort was made along these lines using Parker's alumina method.[24] Our experiments were as follows: The instruments used for the CV measurements were the same as were employed in our foregoing study.[19] In the present experiment, however, positive feedback circuits were added to the above instruments for a so- called IR-drop compensation, though the instruments consist of a three-electrode system.[19,25,26] The CV curves were recorded at various sweep rates. The working electrode was a platinum rod, 1 mm in diameter and sealed in a soft glass tube with a diameter of ca. 6.5 mm.[27] Just before use, we polished the plane head of the platinum electrode with a polishing powder, "Royal Diamond Compound," commercially available. The nonaqueous electrolysis cell used here was the same as that previously reported.[18,19,26,28] A saturated calomel electrode (SCE) was employed as a reference electrode.

**Purification of Solvents.** The solvents for the reduction and oxidation CV measurements were *N,N*-dimethylformamide (DMF) and acetonitrile (AN) respectively, in which 0.1 mol dm$^{-3}$ of tetrapropylammonium perchlorate (TPAP) had been dissolved as a supporting electrolyte. The purification of DMF (Dotite Spectrosol) was carefully done by the method recommended by Juillard;[29] i. e. the impurities were removed by treatment with $P_2O_5$, KOH, and picric acid, its distillation always being carried out in reduced pressure under a nitrogen atmosphere. Just after the purification, we used the DMF for our experiments. AN of Dotite Spectrosol was first treated overnight with $CaH_2$ and then distilled, all the operations being done in a stream of $N_2$.[19,26] According to the method of Hammerich and Parker,[24] the AN was then passed through a column of a neutral alumina (Woelm W 200, active-grade Super I; water addition, 0%; ICN Biomedicals) into the vessel under an $N_2$ atmosphere.

**Experimental Procedure.** The sample solutions were prepared as follows. The necessary amounts of the samples and TPAP were weighed into a 20-ml volumetric flask; then the flask as well as a nonaqueous electrolysis cell were dried overnight in a vacuum desiccator. In a dry box completely filled with $N_2$ gas, the samples in the flask were dissolved with DMF or AN, and then transferred into the electrolysis cell, containing about 10 g of the above neutral alumina, a good suspension of which is required, before recording the CV curves. All the measurements were carried out at 25±0.1 °C at a concentration of 0.5—1×10$^{-3}$ mol dm$^{-3}$. The dissolved oxygen was removed by bubbling $N_2$ gas through the sample solution, and then the inactive gas was passed over the solution surface during the measurement. The trace of moisture in the $N_2$ gas was removed by immersing the $N_2$-gas guide tube into a liquid-nitrogen bath. The method of purifying TPAP was the same as previously reported.[18,19,26,28] The neutral alumina was always kept in a nitrogen atmosphere.

**Samples.** The hydrocarbons employed in the present study are listed in Table 1. All of them were commercially available from Aldrich and Wako Chemical Co. The samples were recrystallized several times from ether, methanol, ethanol, benzene, benzene plus ethanol, benzene plus methanol, and toluene for Samples No. (**1**), (**2**), (**5**,**6**,**10**,**13**), (**7**,**12**), (**3**), (**11**), and (**9**) respectively.[30] High-vacuum sublimation was also used to purify Samples **3**, **4**, **8**, and **9**. All the melting points agreed well with those in the literature, and the elemental analyses of all the samples were in good agreement with the calculated values.

## MO Calculation

In order to interpret the relations between $E^{red}_{1/2\cdot1}$ and $E^{red}_{1/2\cdot2}$ and also between $E^{oxd}_{1/2\cdot1}$ and $E^{oxd}_{1/2\cdot2}$ values, MO calculations were carried out by using the methods of Pariser–Parr–Pople (PPP), CNDO/2, and the ab initio STO-3G basis set for closed shell systems, such as neutral molecules and their dianions and dications.[31,32] In the case of monoanion and monocation radicals in their doublet ground states, we have applied a restricted Longuet-Higgins-Pople type open-shell SCFMO (LP-SCFMO) calculation for π-electron systems.[33,34] The molecular geometries of BAH were determined using the Nishimoto-Forster equation,[35] $r_{cc}=1.517-0.180P_{cc}$, where $r_{cc}$ and $P_{cc}$ are the bond distance and the π-bond order on the nearest neighbor carbon atoms. PPP calculations of neutral species started from the regular hexagon of $r_{cc}=1.396$ Å. After repeating the calculation, final $r_{cc}$ values in the self-consistent as regards $P_{cc}$ were obtained. In this case, the bond angles were altered within 120±2° so as to keep the molecular symmetry.[36] In the PPP- and LP-SCFMO calculations, Nishimoto-Mataga's equation[37] was employed for the evaluation of the two-center-repulsion-integrals, and the core resonance integral, $\beta^{core}_{cc}$, was fixed as −2.37 eV for the sake of convenience.[36] The total energies were calculated using the CNDO/2 and ab initio STO-3G methods. The PPP calculation was carried out with an NEC PC-9801 microcomputer, but the other calculations were performed with the FACOM M-382 and HITAC M-680H computers in the Nagoya University Computation Center and the Okazaki Institute for Molecular Science respectively.

## Results and Discussion

**Theoretical Correlation of the First and Second Half-Wave Potentials Pertinent to Reversible Reduction or Oxidation Processes.** In the foregoing paper we discussed the physical meaning of $E^{red}_{1/2\cdot2}$, $(E^{red}_{1/2\cdot1}+E^{red}_{1/2\cdot2})$, and $(E^{red}_{1/2\cdot1}-E^{red}_{1/2\cdot2})$ from the points of view of the thermodynamical energy cycle and the MO calculation, and also by referring to the derivation of Eq. 1. Equations 3—5 were thus obtained:[19]

$$FE^{red}_{1/2\cdot2}(R^{=}/R^{-}) = \Delta G^{\circ} - \varepsilon^{-}_{so} - \gamma^{-}_{ss} - \Delta E^{=}_{solv} \qquad (3)$$

$$F(E^{red}_{1/2\cdot1} + E^{red}_{1/2\cdot2}) = 2\Delta G^\circ - (\varepsilon^-_{so}+\varepsilon_{1u}+\gamma^-_{ss}) - (\Delta E^-_{solv}+\Delta E^=_{solv}) \quad (4)$$

$$F(E^{red}_{1/2\cdot1} - E^{red}_{1/2\cdot2}) = (\varepsilon^-_{so}-\varepsilon_{1u}+\gamma^-_{ss}) + (\Delta E^=_{solv}-\Delta E^-_{solv}) \quad (5)$$

where the electronic structures of neutral species, monoanion, and dianion are considered separately, $\varepsilon_{lu}$ and $\varepsilon^-_{so}$ being the LUMO and SOMO (singly occupied MO) energies for neutral and anion radical species respectively. The Coulomb-repulsion integral caused by the two electrons in the SOMO of a monoanion is written as $\gamma^-_{ss}$. The solvation energy terms, $\Delta E^=_{solv}$, $(\Delta E^=_{solv}-\Delta E^-_{solv})$, and $(\Delta E^-_{solv}+\Delta E^=_{solv})$, are given by $(E^=_{solv}-E^-_{solv})$, $(E^=_{solv}+E_{solv}-2E^-_{solv})$, and $(E^=_{solv}-E_{solv})$ respectively.[38] Equation 4 is very important for evaluating the solvation energy of a dianion (see below), and Eq. 5 is in intimate correlation with the disproportionation equilibrium of a monoanion, as Hush and Blackledge pointed out qualitatively.[20] In this paper we have newly established the mutual relation of the first and the second half-wave oxidation potentials, $E^{oxd}_{1/2\cdot1}$ and $E^{oxd}_{1/2\cdot2}$, by applying a Born-Haber-type thermodynamical cycle. The $E^{oxd}_{1/2\cdot1}$ value for a reversible redox couple is expressed by Eq. 2, where the energy level is put in vacuo. The energy ($IE^+$) necessary to produce a dication from a monocation can now be represented by the orbital approximation as $IE^+=-\varepsilon^+_{so}-\varepsilon_{coul}$; here, $\varepsilon^+_{so}$ is the SOMO energy of the monocation radical, while $-\varepsilon_{coul}$ is the extra energy needed in order to eject an electron from the cation species by overcoming the Coulomb-stabilization energy, $\varepsilon_{coul}$, between the electron and the cationic core field. This $-\varepsilon_{coul}$ term may be put equal to the two-center-repulsion integral, $\gamma^+_{ss}$, using SOMO, as the CNDO/2 semiempirical theory adopted this model also. Thus, $IE^+=-\varepsilon^+_{so}+\gamma^+_{ss}$; also, the $IE^+$ should correspond to the LUMO energy, $\varepsilon^{++}_{lu}$, of the singlet dication from the point of view of the orbital approximation. The solvation energy term, $\Delta E^{++}_{solv}$, is now given by $\Delta E^{++}_{solv}=E^{++}_{solv}-E^+_{solv}$, $E^{++}_{solv}$ being the solvation energy of the dication. $E^{oxd}_{1/2\cdot2}$ is thus written as Eq. 6 with reference to the derivation of Eq. 2:

$$FE^{oxd}_{1/2\cdot2}(R^{++}/R^+) = \Delta G^\circ - (\varepsilon^+_{so}-\gamma^+_{ss}) + \Delta E^{++}_{solv} \quad (6)$$

The combination of Eqs. 6 and 2 leads to:

$$F(E^{oxd}_{1/2\cdot1} + E^{oxd}_{1/2\cdot2}) = 2\Delta G^\circ - (\varepsilon_{ho}+\varepsilon^+_{so}-\gamma^+_{ss}) + (\Delta E^+_{solv}+\Delta E^{++}_{solv}) \quad (7)$$

and:

$$F(E^{oxd}_{1/2\cdot2}-E^{oxd}_{1/2\cdot1}) = (\varepsilon_{ho}-\varepsilon^+_{so}+\gamma^+_{ss}) + (\Delta E^{++}_{solv}-\Delta E^+_{solv}) \quad (8)$$

The same consideration as is given in Eqs. 3—5 indicates that the solvation energy terms in Eqs. 7 and 8 are given by $(\Delta E^+_{solv}+\Delta E^{++}_{solv})=(E^{++}_{solv}-E_{solv})$ and $(\Delta E^{++}_{solv}-\Delta E^+_{solv})=(E^{++}_{solv}+E_{solv}-2E^+_{solv})$. The physical meaning of Eqs. 7 and 8 is the same as that of Eqs. 4 and 5 except that the former is for the cation species. Equation 7 is especially important for estimating the solvation energy of the dication.

**Correlation between Orbital Energy Approximation and Overall Calculations.** Here it should be pointed out that $(\gamma^+_{ss}-\varepsilon_{ho}-\varepsilon^+_{so})$ in Eq. 7 is equivalent to the $(E^{++}_t-E_t)$, where $E^{++}_t$ and $E_t$ are the total energies of the dication and the neutral molecules respectively. This is because, under Koopmans' theorem,[39] $IE=-\varepsilon_{ho}$, and $IE^+=\gamma^+_{ss}-\varepsilon^+_{so}$ are the quantities pertinent to the total energy difference, expressed by $(E^+_t-E_t)$ and $(E^{++}_t-E^+_t)$ respectively.[19] Similarly, $(\varepsilon^+_{so}-\gamma^+_{ss})$ should correspond to $\varepsilon^{++}_{lu}$, which is the LUMO energy derived from the overall calculation of the dication. The correlation of the $(\gamma^+_{ss}-\varepsilon_{ho}-\varepsilon^+_{so})$ to $(E^{++}_t-E_t)$, and also that of $(\varepsilon^+_{so}-\gamma^+_{ss})$ to $\varepsilon^{++}_{lu}$, were checked by the actual MO calculation of the present BAH's. The total energy values were obtained by the use of the CNDO/2 and ab initio STO-3G methods, while the other quantities were evaluated by means of the PPP-SCF and LP-SCF methods (vide supra). All the calculation results are listed in Table 1. The application of the least-squares method led to the following results:

$$\varepsilon^{++}_{1u} = 0.852(\varepsilon^+_{so}-\gamma^+_{ss}) - 0.104 \quad (9)$$

with $r$ (correlation coefficient) = 0.998 for $n$=11 (Compounds **1**—**11**).

$$(E^{++}_t-E_t) = a(\gamma^+_{ss}-\varepsilon_{ho}-\varepsilon^+_{so}) - c \quad (10)$$

with $a$=1.749, $c$=16.961, $r$=0.988 ($n$=11, Compounds **1**—**11**) for the CNDO/2 total energies, and with $a$=1.366, $c$=17.526, and $r$=0.986 ($n$=10, Compounds **1**—**11** except **5**) for the STO-3G calculation. As was discussed in the foregoing paper,[19] we have similarly obtained Eqs. 11 and 12:

$$\varepsilon^=_{ho} = 0.852(\varepsilon^-_{so}+\gamma^-_{ss}) - 1.655 \quad (11)$$

with $r$=0.998 for 11 compounds **1**—**11** and:

$$(E^=_t-E_t) = a(\varepsilon_{1u}+\varepsilon^-_{so}+\gamma^-_{ss}) + c \quad (12)$$

with $a$=1.546, $c$=6.538, and $r$=0.977 ($n$=11, Compounds **1**—**11**) for the CNDO/2 calculation, and with $a$=1.454, $c$=13.617, and $r$=0.985 ($n$=10, Compounds **1**—**11** except **5**) for the STO-3G calculation. The mutual correlation shown in Eqs. 9—12 is surprisingly good despite the adoption of different calculation methods, indicating that the orbital approximation employed here is quite good for the present systems. It may also be noted that the relations of Eqs. 9—12 are especially good for such polyacenes as Substances **1**—**4**, the correlation coefficient for these cases being more than 0.99976.

Table 1. The Values of the Orbital Energies ($\varepsilon$) and Two-Center-Repulsion Integrals ($\gamma$) Obtained by PPP-Type Approximation for Neutral and Ion Species, and the Total Energy ($E_t$) Differences between Neutral and Ion Species, as Calculated by CNDO/2 and STO-3G Methods on Benzenoid Hydrocarbons[a)]

| No. | Compound | $\varepsilon_{ho}$[b)] | $\varepsilon_{1u}$[c)] | $\varepsilon_{so}^{-}$[d)] | $\gamma_{ss}^{-}$[e)] ($\gamma_{ss}^{+}$)[l)] | $\varepsilon_{ho}^{=}$[f)] | $\varepsilon_{so}^{+}$[g)] | $\varepsilon_{1u}^{++}$[h)] | $\varepsilon_{so}^{-}-\varepsilon_{1u}$ ($\varepsilon_{ho}-\varepsilon_{so}^{+}$)[l)] | $\varepsilon_{so}^{-}+\gamma_{ss}^{-}-\varepsilon_{1u}$ ($\varepsilon_{ho}-\varepsilon_{so}^{+}+\gamma_{ss}^{+}$)[l)] | $\varepsilon_{ho}^{=}-\varepsilon_{1u}$ ($\varepsilon_{ho}-\varepsilon_{1u}^{++}$)[l)] | $E_t^{=}-E_t$[i,j)] | $E_t^{++}-E_t$[i,k)] |
|---|---|---|---|---|---|---|---|---|---|---|---|---|---|
| **1** | Naphthalene | −9.4819 | −2.3581 | −0.1487 | 4.5571 | 2.0818 | −11.6913 | −13.9218 | 2.2094 | 6.7665 | 4.4399 | 9.2353 | 27.6907 |
| | | | | | | | | | | | | (16.2989) | (17.3765) |
| **2** | Anthracene | −8.8272 | −3.0128 | −1.1100 | 4.0332 | 0.7942 | −10.7299 | −12.6341 | 1.9028 | 5.9360 | 3.8070 | 5.9961 | 23.9056 |
| | | | | | | | | | | | | (13.2244) | (14.4799) |
| **3** | Naphthacene | −8.4152 | −3.4248 | −1.7274 | 3.6959 | −0.0374 | −10.1126 | −11.8025 | 1.6974 | 5.3933 | 3.3874 | 3.8021 | 21.4333 |
| | | | | | | | | | | | | (11.1659) | (12.5183) |
| **4** | Pentacene | −8.1454 | −3.6945 | −2.1496 | 3.4416 | −0.6184 | −9.6904 | −11.2216 | 1.5449 | 4.9865 | 3.0761 | 2.2299 | 19.8724 |
| | | | | | | | | | | | | (9.6903) | (11.1014) |
| **5** | Phenanthrene | −9.3915 | −2.4485 | −0.5684 | 4.0326 | 1.2953 | −11.2716 | −13.1353 | 1.8801 | 5.9127 | 3.7438 | 8.2488 | 26.3596 |
| **6** | Benz[*a*]-anthracene | −8.9179 | −2.9220 | −1.2098 | 3.7529 | 0.4736 | −10.6302 | −12.3136 | 1.7122 | 5.4651 | 3.3956 | 5.9962 | 23.7719 |
| | | | | | | | | | | | | (13.0973) | (14.3124) |
| **7** | Chrysene | −9.1027 | −2.7373 | −1.0691 | 3.6339 | 0.5786 | −10.7709 | −12.4185 | 1.6682 | 5.3021 | 3.3159 | 6.7839 | 24.5645 |
| | | | | | | | | | | | | (13.7730) | (14.8412) |
| **8** | Dibenz[*a*,*h*]-anthracene | −8.9553 | −2.8847 | −1.3630 | 3.4277 | 0.1074 | −10.4770 | −11.9473 | 1.5217 | 4.9494 | 2.9921 | 5.8799 | 23.5113 |
| | | | | | | | | | | | | (12.8313) | (14.0020) |
| **9** | Perylene | −8.5180 | −3.3220 | −1.7119 | 3.4588 | −0.0999 | −10.1281 | −11.7401 | 1.6101 | 5.0689 | 3.2221 | 4.3019 | 21.8273 |
| | | | | | | | | | | | | (11.4477) | (12.8763) |
| **10** | Pyrene | −8.8265 | −3.0135 | −1.2082 | 3.7738 | 0.6031 | −10.6318 | −12.4430 | 1.8053 | 5.5791 | 3.6166 | 6.0627 | 23.8771 |
| | | | | | | | | | | | | (13.1492) | (14.4643) |
| **11** | Benzo[*a*]pyrene | −8.5683 | −3.2717 | −1.6517 | 3.5229 | −0.0407 | −10.1883 | −11.7993 | 1.6200 | 5.1429 | 3.2311 | 4.6095 | 22.1943 |
| | | | | | | | | | | | | (11.7603) | (13.1310) |
| **12** | Coronene | −9.0237 | −2.8163 | — | — | — | — | — | — | — | — | — | — |
| **13** | 9,10-Dimethyl-anthracene[m)] | −8.6063 | −2.8547 | −0.9948 | 3.9211 (3.9743)[m)] | 0.8693 | −10.4735 | −12.3430 | 1.8599 (1.8672)[m)] | 5.7811 (5.8415)[m)] | 3.7240 (3.7366)[m)] | 5.5455 | 22.3678 |

a) All the values are in eV units. b) HOMO energy of neutral species. c) LUMO energy of neutral species. d) SOMO energy of monoanion species. e) Values at SOMO calculated by the Nishimoto-Mataga equation for anion and cation species, both of which values come out the same because of the pairing theorem (see text). f) HOMO energy of dianion species. g) SOMO energy of monocation species. h) LUMO energy of dication speies. i) Ab initio STO-3G values are given in parentheses. j) Total energy difference between dianion and neutral species. k) Total energy difference between dication and neutral species. l) These values are the same for the cation and anion species because of the MO-pairing property (see text). m) The MO-pairing theorem is broken for this compound. The values in parentheses are for the energies given in the parentheses in the title.

**Examination of the First and Second Reduction Potentials of Benzenoid Alternant Hydrocarbons by Means of MO Calculations.** When we use the experimental method employed here, reversible or quasireversible reduction voltammograms for all the BAH's, except for naphthalene and phenanthrene, have been recorded not only for the first wave, but also for the second reduction wave under the voltage sweep rates of 50 mV $s^{-1}$—250 V $s^{-1}$, in depending on the substance. However, only the first reduction wave was observed as a reversible voltammogram on naphthalene and phenanthrene. An example of cyclic voltammograms is illustrated in Fig. 1 for perylene. The reversible half-wave reduction potentials were determined using the equation $E^{red}_{1/2}=(E_{cp}+E_{ap})/2$, where $E_{cp}$ and $E_{ap}$ are the cathodic and anodic peak potentials of a CV curve. All of these experimental data are listed in Table 2.[27] It should be noted that the $E^{red}_{1/2\cdot1}$ and $E^{red}_{1/2\cdot2}$ values listed in Table 2 are consistent with those reported by Jensen and Parker[40] for Compounds **2**, **6**, **7**, **9**, and **12**, though their data were obtained at 11 °C and with 0.2 mol $dm^{-3}$ tetramethylammonium bromide as the supporting electrolyte.[41]

Let us now discuss the application of Eqs. 1, 3, 4, and 5 to the present experimental results. As has already been reported by other authors,[6,13–15,17] the

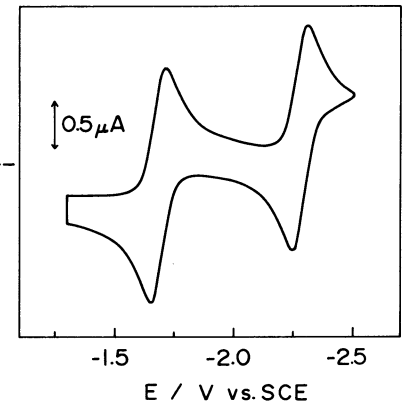


Fig. 1. Cyclic voltammogram of perylene in reduction process at a Pt electrode. Solvent is DMF containing 0.1 mol $dm^{-3}$ TPAP and ca. 10 g of neutral alumina, the sample concentration being $9.3\times10^{-4}$ mol $dm^{-3}$. The voltammogran was recorded at $v=$ 50 mV $s^{-1}$ and 25 °C.

Table 2. First and Second Reduction and Oxidation Potentials, Ionization Potentials, and Electron Affinities of Benzenoid Hydrocarbons

| No. | Compound | Reduction potential[a] (V vs. SCE) | | Oxidation potential[b] (V vs. SCE) | | | | | |
|---|---|---|---|---|---|---|---|---|---|
| | | $E^{red}_{1/2\cdot1}$ | $E^{red}_{1/2\cdot2}$ | $E^{oxd}_{1/2\cdot1}$ | $E^{oxd}_{1/2\cdot2}$ | $(E^{oxd}_{1/2\cdot1}+E^{red}_{1/2\cdot1})/2$ | $I_P$/eV[c] | $E_A$/eV[d] | $(I_P+E_A)/2$ |
| **1** | Naphthalene | −2.557 | — | —[e] | — | — | 8.15 | 0.152 | 4.151 |
| **2** | Anthracene | −1.985 | −2.740 | 1.321 | 1.76 | −0.332 | 7.47 | 0.552 | 4.011 |
| **3** | Naphthacene | −1.595 | −2.245 | 0.980 | 1.47 | −0.308 | 7.04 | — | — |
| **4** | Pentacene | −1.325 | −1.910 | —[f] | — | — | 6.74 | — | — |
| **5** | Phenanthrene | −2.480 | — | —[e] | — | — | 7.86 | 0.308 | 4.084 |
| **6** | Benz[*a*]-anthracene | −2.028 | −2.687 | 1.388 | 1.90 | −0.320 | 7.47 | 0.696 | 4.083 |
| **7** | Chrysene | −2.295 | −2.870 | 1.587 | 2.02 | −0.354 | 7.60 | 0.419 | 4.010 |
| **8** | Dibenz[*a*,*h*]-anthracene | −2.068 | −2.628 | 1.425 | 1.80 | −0.322 | 7.38 | — | — |
| **9** | Perylene[h] | −1.686 (−1.692) | −2.281 (−2.246) | 1.040 | 1.59 | −0.323 (−0.326) | 7.00 | — | — |
| **10** | Pyrene | −2.089 | −2.792 | 1.283 | — | −0.403 | 7.41 | 0.579 | 3.995 |
| **11** | Benzo[*a*]-pyrene | −1.865 | −2.510 | 1.160 | 1.61 | −0.353 | 7.12 | — | — |
| **12** | Coronene | −2.078 | −2.695 | 1.350 | —[g] | −0.364 (−0.342± 0.030)[i] | 7.36 | — | — (4.056± 0.061)[i] |
| **13** | 9,10-Dimethyl-anthracene | −2.002 | −2.708 | 1.098 | 1.538 | −0.452 | — | — | — |

a) These values were obtained from reversible or quasireversible CV curves using a Pt electrode in DMF containing 0.1 mol $dm^{-3}$ TPAP. b) These values were obtained by CV measurements with a Pt electrode in AN containing 0.1 mol $dm^{-3}$ TPAP. Although the first oxidation waves are reversible or quasireversible, the second ones are irreversible for all the samples employed except for Compound **13**, which gave a quasireversible one. See text for the method of evaluating $E^{oxd}_{1/2\cdot2}$. c) Ionization potentials.[52] d) Electron affinities.[43] e) The first oxidation wave was irreversible at $v<200$ V $s^{-1}$. f) Insoluble in AN. g) Three or four oxidation waves were observed. h) Reduction potentials were also measured in AN containing 0.1 mol $dm^{-3}$ TPAP. These are given in parentheses. i) Average values are given in parentheses.

data in Tables 1 and 2 indicate a good linear relation to satisfy Eq. 1, written as $E^{red}_{1/2\cdot1}=-0.895\varepsilon_{lu}-4.681$, with $r=0.985$ and $n=12$ (Compounds **1—12**). The absolute value (0.895) of the slope is near to the theoretical value of unity. The first reduction potential, $E^{red}_{1/2\cdot1}$, is then well expressed by Eq. 1.[42,43] We next test Eq. 3 again using the data in Tables 1 and 2. The $E^{red}_{1/2\cdot2}$ vs. $(\varepsilon^{-}_{so}+\gamma^{-}_{ss})$ plot is $E^{red}_{1/2\cdot2}=-0.549\ (\varepsilon^{-}_{so}+\gamma^{-}_{ss})-1.327$, with $r=0.897$ and $n=9$ (Compounds **2—4, 6—11**). Since $\varepsilon^{=}_{ho}$ is in a good correlation with $(\varepsilon^{-}_{so}+\gamma^{-}_{ss})$, as may be understood from Eq. 11, we attempted to establish the plot of $E^{red}_{1/2\cdot2}$ against $\varepsilon^{=}_{ho}$; it is illustrated in Fig. 2 along with the correlation equation.[44] The above linearity seems to be relatively good, but the absolute values of the slope and the correlation coefficients are both smaller than those of the $E^{red}_{1/2\cdot1}$ vs. $\varepsilon_{lu}$ plot. As would be expected, one of these factors may be attributed to the lower accuracy of the orbital-energy calculations of the mono- and dianion species in comparison with those of the neutral one. However, another important reason is the different contribution from the molecular electronic states and the solvation-energy terms between the redox systems of $R+e\rightleftarrows R^{-}$ (Eq. 1) and $R^{-}+e\rightleftarrows R^{=}$ (Eq. 3). It is well known that the π-electron distribution on each carbon atom in neutral alternant hydrocarbon is the same,[45] so that their π-dipole moment is zero, thus leading to a small solute-solvent interaction. However, generally speaking, the electron density of the anion radical of BAH is not uniformly distributed in the molecules,[46] because π-electrons in the LUMO are distributed mainly over the atomic orbitals determined by its orbital symmetry.[44] This tendency turns out to be much larger for the dianion than for the monoanion, so the possibility of a specific solute (ion)-solvent interaction seems to be larger for the former than the latter.[47] This must play an important role for that the correlation coefficient of the $E^{red}_{1/2\cdot2}$ vs. $(\varepsilon^{-}_{so}+\gamma^{-}_{ss})$ or $\varepsilon^{=}_{ho}$ plot is less than that of the $E^{red}_{1/2\cdot1}$ vs. $\varepsilon_{lu}$ plot. In addition, the BAH's studied here extend from small-ring-size molecules (small cavity radius in solution) to large ones (large cavity radius). Therefore, a Born-type equation[48] indicates that the contribution from the solvation-energy term is not constant in the strict sense; this tendency is more important in the $E^{red}_{1/2\cdot2}$ step than in the $E^{red}_{1/2\cdot1}$ step (see below). This fact is discussed in the Appendix from the point of view of multivariate analysis. As a result, we can expect a positive correlation of $E^{red}_{1/2\cdot2}$ to $\Delta E^{=}_{solv}$ (Eq. 3). In other words, the values of both $E^{red}_{1/2\cdot2}$ and $\Delta E^{=}_{solv}$ move to a small negative value with an increase in the ring size (vide infra). This may cause the decrease in the slope value of the $E^{red}_{1/2\cdot2}$ vs. $(\varepsilon^{-}_{so}+\gamma^{-}_{ss})$ or $\varepsilon^{=}_{ho}$ plot.

Let us now turn to a discussion of Eq. 4. Using the linear relations of Eqs. 11 and 12, the plots of $(E^{red}_{1/2\cdot1}+E^{red}_{1/2\cdot2})$ to $(E^{=}_{t}-E_{t})$, $(\varepsilon_{lu}+\varepsilon^{=}_{ho})$, and $(\varepsilon_{lu}+\varepsilon^{-}_{so}+\gamma^{-}_{ss})$ led to good linear relations as follows: $(E^{red}_{1/2\cdot1}+E^{red}_{1/2\cdot2})=-a(E^{=}_{t}-E_{t})-b$ with $a=0.417$ (0.459), $b=2.287$ (−1.212), and $r=0.990$ (0.987) for the CNDO/2 and ab initio STO-3G calculations (the latter is given in parentheses); $(E^{red}_{1/2\cdot1}+E^{red}_{1/2\cdot2})=-0.808(\varepsilon_{lu}+\varepsilon^{=}_{ho})-6.781$ with $r=0.962$; $(E^{red}_{1/2\cdot1}+E^{red}_{1/2\cdot2})=-0.734(\varepsilon_{lu}+\varepsilon^{-}_{so}+\gamma^{-}_{ss})-5.113$ with $r=0.942$. The compounds employed are Nos. **2—4** and **6—11**. An example is illustrated in Fig. 3. We think that the theoretical Eq. 4 is quite well satisfied from the experimental point of view. The relatively large difference in the slope values between the orbital-energy approximation and the total energy calculations may be attributed to the different models adopted here; i. e., the "*a*" value of Eq. 12 shows large deviation from 1.

Let us next consider the physical meaning of the $(E^{red}_{1/2\cdot1}-E^{red}_{1/2\cdot2})$ given by Eq. 5, where we can easily understand that the $\gamma^{-}_{ss}$ values make the largest

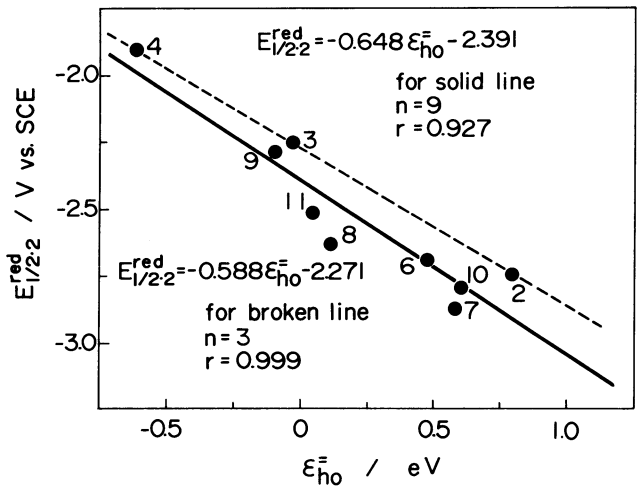


Fig. 2. Linear relation of $E^{red}_{1/2\cdot2}$ values to $\varepsilon^{=}_{ho}$ for BAH's. Each sample number is the same as given in Table 1. See text for detail.

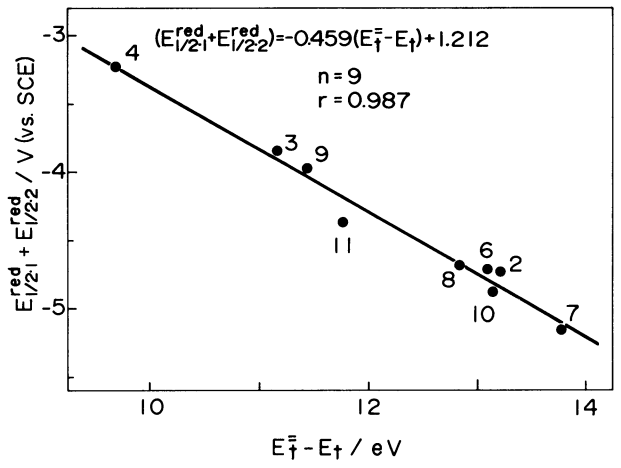


Fig. 3. Linear relation of $(E^{red}_{1/2\cdot1}+E^{red}_{1/2\cdot2})$ values to $(E^{=}_{t}-E_{t})$ calculated by ab initio STO-3G method for BAH's. Each sample number is the same as given in Table 1. See text for detail.

contribution to $(E^{red}_{1/2\cdot1}-E^{red}_{1/2\cdot2})$, as Hush and Blackledge[20] first pointed out, for if all the energy discussions are made for neutral molecules, $(\varepsilon^{-}_{so}-\varepsilon_{lu})=0$. Now it should be noted that the $\Delta G°$ term does not appear in Eq. 5, and the solvation energy term $(\Delta E^{=}_{solv}-\Delta E^{-}_{solv}$: negative value) cancels out the contribution from the orbital energy term $(\gamma^{-}_{ss}+\varepsilon^{-}_{so}-\varepsilon_{lu}$: positive value), so that, as may be seen in Fig. 4, the value of $(E^{red}_{1/2\cdot1}-E^{red}_{1/2\cdot2})$ becomes small and varies within a smaller range than in the structure change of $(\gamma^{-}_{ss}+\varepsilon^{-}_{so}-\varepsilon_{lu})$, in which $\gamma^{-}_{ss}$ makes the largest contribution (see Table 1).[49,50] This fact seems to be the main reason why the slope of the $(E^{red}_{1/2\cdot1}-E^{red}_{1/2\cdot2})$ vs. $(\gamma^{-}_{ss}+\varepsilon^{-}_{so}-\varepsilon_{lu})$ plot becomes small.

**Examination of the First and Second Oxidation Potentials of Benzenoid Alternant Hydrocarbons by Means of MO Calculations.** Under the experimental conditions described above, the voltammetric study of the oxidation processes in AN using a platinum electrode shows that, although a reversible or quasireversible oxidation CV curve is recorded in the first oxidation process by selecting a suitable voltage-scan rate of 0.1—60 V $s^{-1}$, we could not succeed in obtaining a reversible or a quasireversible CV curve for the second oxidation process. An example is given in Fig. 5 for perylene. These experimental results show that the dications of BAH are more unstable than the dianions. However, note that if the strongly reactive 9- and 10-positions of anthracene are protected by $CH_3$ substitution, a reversible CV curve is safely recorded for both the first and second oxidation steps (see Table 2). The standard potential of the first oxidation step was evaluated by the use of $E^{oxd}_{1/2\cdot1}=(E'_{ap\cdot1}+E'_{cp\cdot1})/2$, where the superfix (′) of $E_{ap\cdot1}$ and $E_{cp\cdot1}$ indicates the first oxidation system. In the case of the second oxidation step, $E^{oxd}_{1/2\cdot2}$ was estimated by means of the $E^{oxd}_{1/2\cdot2}=E'_{ap\cdot2}-(E'_{ap\cdot1}-E^{oxd}_{1/2\cdot1})$ equation, which indicates that the $E^{oxd}_{1/2\cdot2}$ value occupies a position less positive than $E'_{ap\cdot2}$ by the same amount as $(E'_{ap\cdot1}-E^{oxd}_{1/2\cdot1})$ relative to the quasireversible first oxidation CV curve (see Fig. 5). For this treatment to get $E^{oxd}_{1/2\cdot2}$, we have employed the CV data at the sweep rate of $v$, where the $(E'_{ap\cdot2}-E'_{ap\cdot1})$ value becomes almost independent of an increasing $v$. At this scan rate, it appears reasonable to assume that an electron-transfer step at the electrode may play an important role in determining $E^{oxd}_{1/2\cdot2}$,[51] but the effect from succeeding chemical reactions may be diminished. All these experimental results are included in Table 2. As was reported by earlier workers,[14,15,17] the correlation of the $E^{oxd}_{1/2\cdot1}$ vs. $\varepsilon_{ho}$ plot is quite good, as $E^{oxd}_{1/2\cdot1}=-0.770\varepsilon_{ho}-5.493$, with $r=0.963$ and $n=9$ (Compounds **2**, **3**, **6—12**). Only coronene deviates from the straight line, so when we delete it from the plotting the values of 0.989, −0.849, and −6.083 were obtained for the $r$, the slope, and the constant term respectively. If we use the vertical ionization potential ($I_P$) reported by Clar et al.[52] in lieu of the $-\varepsilon_{ho}$, the equation of $E^{oxd}_{1/2\cdot1}=0.853I_P-4.961$ is obtained, with $r=0.938$ and $n=9$. The slope is compatible with that of the $E^{oxd}_{1/2\cdot1}$ vs. $\varepsilon_{ho}$ plot.[53] To examine Eq. 6, the mutual relation of $E^{oxd}_{1/2\cdot2}$ and $(\varepsilon^{+}_{so}-\gamma^{+}_{ss})$ was studied. The result is $E^{oxd}_{1/2\cdot2}=-0.528(\varepsilon^{+}_{so}-\gamma^{+}_{ss})-5.636$, with $r=0.875$ and $n=6$ (Compounds **3**, **6—9**, **11**), but if $\varepsilon^{++}_{lu}$ is employed in place of $(\varepsilon^{+}_{so}-\gamma^{+}_{ss})$, we obtain the results illustrated in Fig. 6. Here, anthracene is excluded from the plotting because of its

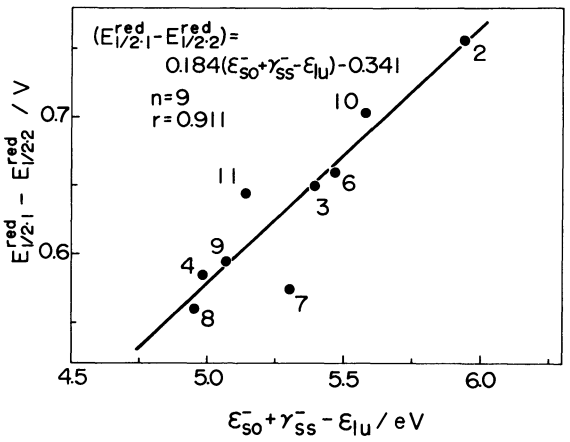


Fig. 4. Linear relation of $(E^{red}_{1/2\cdot1}-E^{red}_{1/2\cdot2})$ values to $(\varepsilon^{-}_{so}+\gamma^{-}_{ss}-\varepsilon_{lu})$ for BAH's. Each sample number is the same as given in Table 1. When $\varepsilon^{=}_{ho}$ is adopted instead of $(\varepsilon^{-}_{so}+\gamma^{-}_{ss})$, the correlation is: $(E^{red}_{1/2\cdot1}-E^{red}_{1/2\cdot2})=0.235(\varepsilon^{=}_{ho}-\varepsilon_{lu})-0.147$ with $r=0.925$.

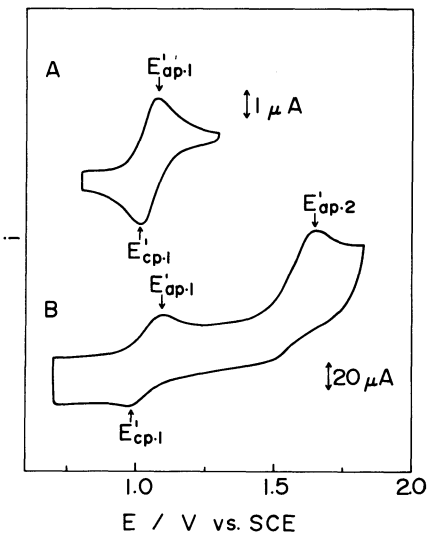


Fig. 5. Cyclic voltammograms of perylene in oxidation process at a Pt electrode. Solvent is AN containing 0.1 mol $dm^{-3}$ TPAP and ca. 10 g of neutral alumina, the sample concentration being $1.0\times10^{-3}$ mol $dm^{-3}$. The voltammograms were recorded at $v=0.2$ V $s^{-1}$ for A and 22.4 V $s^{-1}$ for B at 25 °C. $E'_{ap\cdot1}$, $E'_{cp\cdot1}$, and $E'_{ap\cdot2}$ indicate the peak potentials of the first anodic, cathodic, and the second anodic waves, respctively (see text).

large deviation from the linear relation. This deviation should be ascribed to the large reactivity of the 9- and 10-positions of the anthracene dications, so the $E^{oxd}_{1/2\cdot2}$ value is not so accurate as the other values.[54] Just as in the aforementioned $E^{red}_{1/2\cdot2}$ vs. $(\varepsilon^{-}_{so}+\gamma^{-}_{ss})$ correlation, the relation of $E^{oxd}_{1/2\cdot2}$ to $(\varepsilon^{+}_{so}-\gamma^{+}_{ss})$ indicates that, in comparison with the case of the $E^{oxd}_{1/2\cdot1}$ vs. $\varepsilon_{ho}$ plot, the correlation coefficient is not so good and the slope value is small. The same discussion as has been made for interpreting Eq. 3 can also be applied to the present case. In addition, the problem that the reversibility of the second oxidation wave is not sufficient is not neglected here.

Our next discussion will be focused on Eq. 7. The relations of $(E^{oxd}_{1/2\cdot1}+E^{oxd}_{1/2\cdot2})$ to $(\varepsilon_{ho}+\varepsilon^{+}_{so}-\gamma^{+}_{ss})$ or $(\varepsilon_{ho}+\varepsilon^{++}_{lu})$ or $(E_t-E_t^{++})$ are as follows: $(E^{oxd}_{1/2\cdot1}+E^{oxd}_{1/2\cdot2})=-0.714(\varepsilon_{ho}+\varepsilon^{+}_{so}-\gamma^{+}_{ss})-13.229$ with $r=0.957$, $n=6$; $(E^{oxd}_{1/2\cdot1}+E^{oxd}_{1/2\cdot2})=-0.794(\varepsilon_{ho}+\varepsilon^{++}_{lu})-13.477$, with $r=0.979$ and $n=6$; $(E^{oxd}_{1/2\cdot1}+E^{oxd}_{1/2\cdot2})=-0.360(E_t-E_t^{++})-5.246$, with $r=0.999$ and $n=6$ for the CNDO/2 calculation; $(E^{oxd}_{1/2\cdot1}+E^{oxd}_{1/2\cdot2})=-0.492(E_t-E_t^{++})-3.697$, with $r=0.998$ and $n=6$ for the STO-3G calculation. Compounds **3**, **6—9**, **11** were employed for the correlation study. Again, anthracene was omitted from the plotting for the aforementioned reason. An example is shown in Fig. 7. The theoretical Eq. 7 seems to be well satisfied. However, quite a large difference between the total-energy-calculation models and the orbital-energy approximation is found for the slope values of the linear-regression equations. This is the same phenomenon as was observed and discussed in the correlations of $(E^{red}_{1/2\cdot1}+E^{red}_{1/2\cdot2})$ against $(\varepsilon^{-}_{so}+\varepsilon_{lu}+\gamma^{-}_{ss})$ or $(\varepsilon^{=}_{ho}+\varepsilon_{lu})$ or $(E^{=}_{t}-E_t)$ values (vide supra).

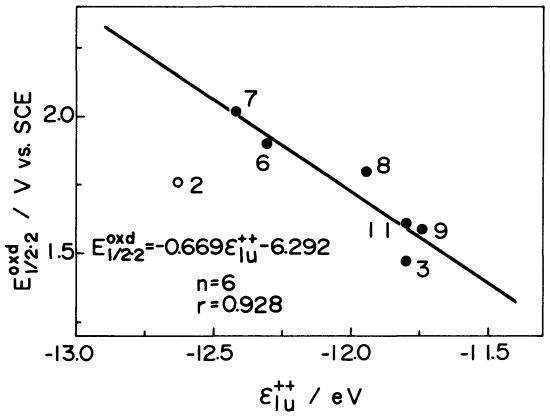


Fig. 6. Linear relation of $E^{oxd}_{1/2\cdot2}$ values to $\varepsilon^{++}_{lu}$ for BAH's. Each sample number is the same as given in Table 1. See text for detail.

Next, let us consider the physical meaning of $(E^{oxd}_{1/2\cdot2}-E^{oxd}_{1/2\cdot1})$ given by Eq. 8, whose form is closely similar to Eq. 5 pertinent to $(E^{red}_{1/2\cdot1}-E^{red}_{1/2\cdot2})$, so that the same discussion as was made for Eq. 5 would be possible. It is well-known that the so-called "pairing property"[45,55] of the MO's obtained by the PPP method holds between occupied and unoccupied MO's of neutral BAH molecules and also between the SOMO or unoccupied MO's of the anion radicals and the SOMO or occupied MO's of the cation radicals. Our present calculations verified this, so the values of $\gamma^{+}_{ss}$ and $(\varepsilon_{ho}-\varepsilon^{+}_{so})$ are equal to $\gamma^{-}_{ss}$ and $(\varepsilon^{-}_{so}-\varepsilon_{lu})$ respectively. As a result, $(\varepsilon_{ho}-\varepsilon^{+}_{so}+\gamma^{+}_{ss})$ and $(\varepsilon^{-}_{so}-\varepsilon_{lu}+\gamma^{-}_{ss})$ are the same value. Also, the present calculations suggest that the values of $(\varepsilon^{=}_{ho}-\varepsilon_{lu})$ and $(\varepsilon_{ho}-\varepsilon^{++}_{lu})$ are equal to each other, because the pairing property found between the anion and cation radicals of BAH again holds between the MO's of the dianion and dication species as well as between the $\varepsilon^{=}_{ho}$ and $\varepsilon^{++}_{lu}$. This can also be inferred from the relations of Eqs. 9 and 11. Keeping in mind the above fact, we can expect that, judging from the comparison of Eqs. 5 and 8, the values of $(E^{oxd}_{1/2\cdot2}-E^{oxd}_{1/2\cdot1})$ should be the same as those of $(E^{red}_{1/2\cdot1}-E^{red}_{1/2\cdot2})$ if (i) the solvation effect on reversible redox potentials is not so different between DMF and

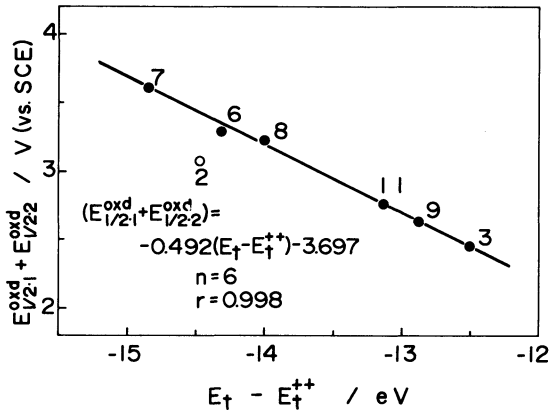


Fig. 7. Linear relation of $(E^{oxd}_{1/2\cdot1}+E^{oxd}_{1/2\cdot2})$ values to $(E_t-E_t^{++})$ calculated by ab initio STO-3G method for BAH's. Each sample number is the same as given in Table 1. See text for detail.

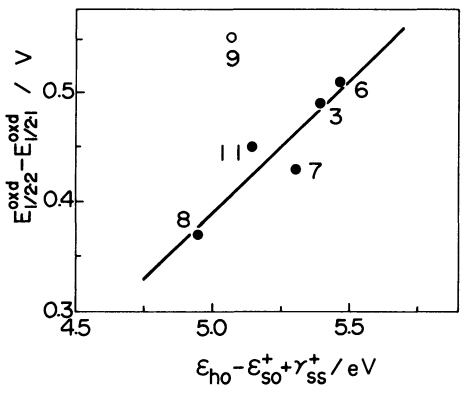


Fig. 8. Linear relation of $(E^{oxd}_{1/2\cdot2}-E^{oxd}_{1/2\cdot1})$ values to $(\varepsilon_{ho}-\varepsilon^{+}_{so}+\gamma^{+}_{ss})$ for BAH's with the slope=0.243, the constant term=−0.826, and $r=0.918$. Each sample number is the same as given in Table 1. See text for detail.

AN[56] and (ii) the solvation energies coming from mono- and dianions are the same as those of the mono- and dications (vide infra). In the present experiments, $E^{red}_{1/2\cdot1}$, $E^{red}_{1/2\cdot2}$, and $E^{oxd}_{1/2\cdot1}$ are for the reversible or quasireversible CV curves, but $E^{oxd}_{1/2\cdot2}$ is not and it is, therefore, less positive than the value in a reversible curve. The one exception is perylene, whose $(E^{oxd}_{1/2\cdot2}-E^{oxd}_{1/2\cdot1})$ value is quite close to the value of $(E^{red}_{1/2\cdot1}-E^{red}_{1/2\cdot2})$, as Table 2 shows, so we suppose that the $E^{oxd}_{1/2\cdot2}$ value of perylene in Table 2 may be near that of a reversible monocation and dication redox system. The correlation of Eq. 8 is: $(E^{oxd}_{1/2\cdot2}-E^{oxd}_{1/2\cdot1})=0.243(\varepsilon_{ho}-\varepsilon^{+}_{so}+\gamma^{+}_{ss})-0.826$, with $r=0.918$ and $n=5$; also, $(E^{oxd}_{1/2\cdot2}-E^{oxd}_{1/2\cdot1})=0.304(\varepsilon_{ho}-\varepsilon^{++}_{lu})-0.543$, with $r=0.922$ and $n=5$. The compounds employed for the correlation are **3**, **6—8**, **11**. Perylene deviates greatly from the above equations, so we have excluded it from the linear plotting, as is shown in Fig. 8. The reason is clear from the discussion above. In turn, for the same reason as was discussed in detail in connection with Eq. 5, the value of $(E^{oxd}_{1/2\cdot2}-E^{oxd}_{1/2\cdot1})$ comes out small and varies in a smaller range than in the case of $(\varepsilon_{ho}-\varepsilon^{+}_{so}+\gamma^{+}_{ss})$, where $\gamma^{+}_{ss}$ makes the largest contribution (see Table 1).[49,50] Therefore, the slope of the $(E^{oxd}_{1/2\cdot2}-E^{oxd}_{1/2\cdot1})$ vs.$(\varepsilon_{ho}-\varepsilon^{+}_{so}+\gamma^{+}_{ss})$ plotting turns out to be small, as was seen in the discussion of Eq. 5.

**Mutual Relation between Standard Reduction and Oxidation Potentials.** In a series of alternant hydrocarbons, it is well-known[45,57] and has been experimentally verified that the sum of $I_P$ and $E_A$ is almost constant. The data shown in Table 2 support this relation, and Mulliken's electro-negativity $((I_P+E_A)/2)$[58] is constant in BAH and is 4.06 eV for the data in Table 2. This kind of property can be well described using just the PPP-SCFMO employed here; i. e., the pairing property of MO is well satisfied. In terms of the MO language employing Koopmans' theorem,[39] $(I_P+E_A)/2$ corresponds to $-(\varepsilon_{ho}+\varepsilon_{lu})/2$ for neutral molecules. The present calculations led to $-5.92$ eV for $(\varepsilon_{ho}+\varepsilon_{lu})/2$ and for the pairing orbitals between anion and cation radicals (e. g., $(\varepsilon^{+}_{so}+\varepsilon^{-}_{so})/2$) and also for those between dianion and dication species (e. g., $(\varepsilon^{++}_{lu}+\varepsilon^{=}_{ho})/2$). When we use Eqs. 1 and 2, the value of $(E^{oxd}_{1/2\cdot1}+E^{red}_{1/2\cdot1})/2$ is written by Eq. 13:

$$(E^{oxd}_{1/2\cdot1}+E^{red}_{1/2\cdot1})/2 = \Delta G^{\circ}-(\varepsilon_{1u}+\varepsilon_{ho})/2+(\Delta E^{+}_{solv}-\Delta E^{-}_{solv})/2 \quad (13)$$

where the eV unit is used for the energies. Taking into consideration the fact that Eqs. 1 and 2 are well fulfilled experimentally, the $\Delta E^{+}_{solv}$ term can be expected to cancel out the $\Delta E^{-}_{solv}$ term, so the term $(E^{oxd}_{1/2\cdot1}+E^{red}_{1/2\cdot1})$ turns out to be constant.[59] The values are listed in Table 2; the average potential is $-0.342\pm0.030$ V. Now, we can estimate the $\Delta G^{\circ}$ from Eq. 13 by putting $\Delta E^{+}_{solv}=\Delta E^{-}_{solv}$ (vide infra). Using the value of 5.92 eV for $-(\varepsilon_{lu}+\varepsilon_{ho})/2$, we obtain $\Delta G^{\circ}=-6.26$ eV.[60] However, when we use $(I_P+E_A)/2$ in place of $-(\varepsilon_{lu}+\varepsilon_{ho})/2$, $\Delta G^{\circ}=-4.40$ eV where we employ $4.056\pm0.061$ eV for the average value of the former (see Table 2). This $\Delta G^{\circ}$ value is reasonable in view of the literature values.[11,61,62] Hereafter, therefore, we will use $\Delta G^{\circ}=-6.26$ eV for PPP orbital treatment, but

Table 3. Calculated Values of Second Oxidation Potential and Solvation Energies of Benzenoid Alternant Hydrocarbons

| No. | Compound | $E^{oxd}_{1/2\cdot2}$(cal)[a] | $E^{-}_{solv}$[b] (eV) | | $E^{+}_{solv}$[c] (eV) | | $E^{=}_{solv}$[d] (eV) | | $E^{++}_{solv}$[e] (eV) | |
|---|---|---|---|---|---|---|---|---|---|---|
| | | V vs. SCE | [A] | [B] | [C] | [D] | [E] | [F] | [G] | [H] |
| **1** | Naphthalene | — | −1.35 | −1.69 | — | — | — | — | — | — |
| **2** | Anthracene | 2.076 | −1.26 | −1.86 | −1.24 | −1.75 | −7.71 | −5.58 | −7.99 | −5.86 |
| **3** | Naphthacene | 1.630 | −1.24 | — | −1.17 | −1.66 | −7.23 | −5.22 | −7.25 | −5.24 |
| **4** | Pentacene | — | −1.24 | — | — | — | −6.89 | −4.98 | — | — |
| **5** | Phenanthrene | — | −1.33 | −1.61 | — | — | — | — | — | — |
| **6** | Benz[*a*]anthracene | 2.047 | −1.31 | −1.67 | −1.27 | −1.68 | −7.43 | −5.36 | −7.49 | −5.42 |
| **7** | Chrysene | 2.162 | −1.23 | −1.68 | −1.25 | −1.62 | −7.19 | −5.20 | −7.37 | −5.39 |
| **8** | Dibenz[*a*,*h*]anthracene | 1.985 | −1.31 | — | −1.27 | −1.56 | −7.01 | −5.05 | −7.11 | −5.15 |
| **9** | Perylene | 1.635 | −1.25 | — | −1.22 | −1.56 | −6.98 | −5.14 | −6.95 | −5.10 |
| **10** | Pyrene | 1.986 | −1.16 | −1.73 | −1.28 | −1.73 | −7.20 | −5.23 | — | — |
| **11** | Benzo[*a*]pyrene | 1.805 | −1.13 | — | −1.15 | −1.56 | −6.75 | −4.84 | −6.99 | −5.07 |
| **12** | Coronene | 1.967 | −1.37 | — | −1.41 | −1.61 | — | — | — | — |

a) Second oxidation potential calculated by means of this equation: $E^{oxd}_{1/2\cdot2}=E^{oxd}_{1/2\cdot1}+E^{red}_{1/2\cdot1}-E^{red}_{1/2\cdot2}$. See text for the details. b) Solvation energy of monoanion species. Calculations were made using Eq. 1; $E^{-}_{solv}\simeq(E^{-}_{solv}-E_{solv})=-FE^{red}_{1/2\cdot1}-\varepsilon_{1u}-6.26$ for [A], but $-FE^{red}_{1/2\cdot1}+E_A-4.40$ for [B]. c) Solvation energy of monocation species. Calculations were made using Eq. 2; $E^{+}_{solv}\simeq(E^{+}_{solv}-E_{solv})=FE^{oxd}_{1/2\cdot1}+\varepsilon_{ho}+6.26$ for [C], but $FE^{oxd}_{1/2\cdot1}-I_P+4.40$ for [D]. d) Solvation energy of dianion species. Calculatations were made using Eq. 4; $E^{=}_{solv}\simeq(E^{=}_{solv}-E_{solv})=-F(E^{red}_{1/2\cdot1}+E^{red}_{1/2\cdot2})-(\varepsilon^{-}_{so}+\gamma^{-}_{ss}+\varepsilon_{1u})-12.52$ for [E], but $-F(E^{red}_{1/2\cdot1}+E^{red}_{1/2\cdot2})-(\varepsilon^{=}_{ho}+\varepsilon_{1u})-12.52$ for [F]. e) Solvation energy of dication species. Calculations were made using Eq. 7; $E^{++}_{solv}\simeq(E^{++}_{solv}-E_{solv})=F(E^{oxd}_{1/2\cdot1}+E^{oxd}_{1/2\cdot2})+(\varepsilon^{+}_{so}-\gamma^{+}_{ss}+\varepsilon_{ho})+12.52$ for [G], but $F(E^{oxd}_{1/2\cdot1}+E^{oxd}_{1/2\cdot2})+(\varepsilon^{++}_{lu}+\varepsilon_{ho})+12.52$ for [H].

−4.40 eV in the consideration of the experimental $I_P$ and $E_A$ values.

Now we would like to discuss the mutual relation between $E^{oxd}_{1/2\cdot2}$ and $E^{red}_{1/2\cdot2}$. Taking the summation of Eqs. 3 and 6, and by dividing it by two, we obtain Eq. 14 (in eV units):

$$(E^{red}_{1/2\cdot2}+E^{oxd}_{1/2\cdot2})/2 = \Delta G^\circ - (\varepsilon^-_{so}+\varepsilon^+_{so})/2 + (\gamma^+_{ss}-\gamma^-_{ss})/2 + (\Delta E^{++}_{solv}-\Delta E^{=}_{solv})/2 \quad (14)$$

The MO-pairing property of the anion and cation PPP-SCFMO for BAH shows that $\gamma^+_{ss}-\gamma^-_{ss}=0$, and $(\varepsilon^+_{so}+\varepsilon^-_{so})/2=(\varepsilon_{ho}+\varepsilon_{lu})/2=-5.92$ eV. Provided that $\Delta E^{++}_{solv}-\Delta E^{=}_{solv}\simeq0$ just like $\Delta E^{+}_{solv}\simeq\Delta E^{-}_{solv}$ in Eq. 13, Eq. 14 comes out to be equal to Eq. 13, -i. e., $(E^{oxd}_{1/2\cdot1}+E^{red}_{1/2\cdot1})=(E^{oxd}_{1/2\cdot2}+E^{red}_{1/2\cdot2})$. Note that $E^{red}_{1/2\cdot1}$, $E^{red}_{1/2\cdot2}$, and $E^{oxd}_{1/2\cdot1}$ were experimentally determined from the reversible or quasireversible CV curves; therefore, we can calculate $E^{oxd}_{1/2\cdot2}$ by employing this equation: $E^{oxd}_{1/2\cdot2}=E^{oxd}_{1/2\cdot1}+E^{red}_{1/2\cdot1}-E^{red}_{1/2\cdot2}$. The calculated values are given in Table 3, while the correlation of the observed $E^{oxd}_{1/2\cdot2}$ values with the calculated values is illustrated in Fig. 9. We can see there that the observed and calculated $E^{oxd}_{1/2\cdot2}$ values, except for perylene and anthracene, fall as a good linear-least-squares correlation line. The observed values are positive-shifted by ≈0.2 V from the calculated values. This is reasonable, since the experimental values were determined from irreversible CV curves. Therefore, the effect of the succeeding chemical reaction on them could not be neglected, but the effect is in the same order in the above five substances. Anthracene deviated largely to the positive side from the regression line, showing that the effect of the following chemical reaction on it is very large; this tendency of anthracene was always found in the present correlation study of the oxidation processes. In turn, Fig. 9 indicates that perylene is in a position close to, but a little positive-shifted from, the theoretical line. Its $E^{oxd}_{1/2\cdot2}$ value should be near to that of the reversible equilibrium; this conclusion is the same as that derived from the foregoing discussion of the $(E^{oxd}_{1/2\cdot2}-E^{oxd}_{1/2\cdot1})$ value.

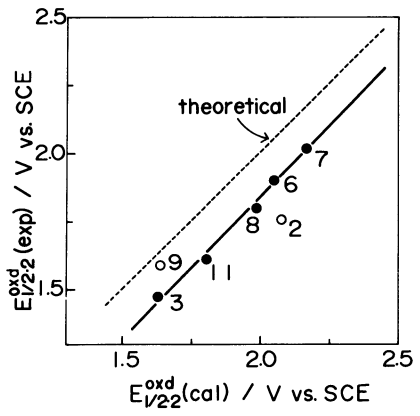


Fig. 9. Linear relation of the experimental $E^{oxd}_{1/2\cdot2}$ values to the calculated $E^{oxd}_{1/2\cdot2}$ ones given in Table 3 for BAH's. Each sample number is the same as given in Table 1. Regression equation is $E^{oxd}_{1/2\cdot2}(exp)=1.049E^{oxd}_{1/2\cdot2}(cal)-0.260$ with $r=0.995$, $n=5$ (full circles). See text for detail.

**Evaluation of Solvation Energies of Ion Species.** Now, let us discuss the solvation energies of anions or cations of BAH by applying Eqs. 1, 2, 4, and 7. From the former two equations, we can estimate the $(E^-_{solv}-E_{solv})\simeq E^-_{solv}$ and $(E^+_{solv}-E_{solv})\simeq E^+_{solv}$ values, and the latter two give the estimated values of $(E^{=}_{solv}-E_{solv})\simeq E^{=}_{solv}$ and $(E^{++}_{solv}-E_{solv})\simeq E^{++}_{solv}$, although the CV reversibility pertinent to the $E^{oxd}_{1/2\cdot2}$ value is not very good. Of course, ΔG° should be −6.26 eV for the PPP-orbital approximation,[60] but −4.40 eV for $I_P$ and $E_A$. The calculated results are listed in Table 3, from which one can conjecture that, in the case of $E^-_{solv}$ and $E^+_{solv}$, the values evaluated from the PPP calculations and the $I_P$ or $E_A$ value are both of almost the same order of magnitude, though the absolute values calculated from the experimental $I_P$ and $E_A$ values are a little larger than in the orbital approximation, and that their structure dependence is small, as is to be expected from the regression equations of the $E^{red}_{1/2\cdot1}$ vs. $\varepsilon_{lu}$ (or $E_A$) and $E^{oxd}_{1/2\cdot1}$ vs. $\varepsilon_{ho}$ (or $I_P$) relationships. On the other hand, the absolute values of $E^{=}_{solv}$ and $E^{++}_{solv}$, as estimated using $\varepsilon^{=}_{ho}$ and $\varepsilon^{++}_{lu}$ in lieu of $(\varepsilon^-_{so}+\gamma^-_{ss})$ and $(\varepsilon^+_{so}-\gamma^+_{ss})$ (see Eqs. 4 and 7), are about 2 eV smaller than those obtained employing $(\varepsilon^-_{so}+\gamma^-_{ss})$ and $(\varepsilon^+_{so}-\gamma^+_{ss})$ directly. This is understandable when we take into consideration the correlation of Eqs. 9 and 11. However, the solvation energies themselves of the dianion or dication calculated using $\varepsilon^{=}_{ho}$ or $\varepsilon^{++}_{lu}$ are more accurate than those obtained from $(\varepsilon^-_{so}+\gamma^-_{ss})$ or $(\varepsilon^+_{so}-\gamma^+_{ss})$, because the latter values are for the orbital approximation to the former values, derived from the overall MO calculation, just like the $\varepsilon_{lu}$ or $\varepsilon_{ho}$ in Eqs. 1 and 2. Now, in comparing the solvation energies of the dianion and dication with those of the monoanion and monocation under the same calculation models, we can see in Table 3 that $|E^{=}_{solv}|=4.2(\pm0.2)|E^-_{solv}|$ for Columns F and A and $|E^{++}_{solv}|=4.3(\pm0.2)|E^+_{solv}|$ for Columns H and C. In addition, the change in $|E^{=}_{solv}|$ with the ring size seems to be in a reasonable direction; e. g., $|E^{=}_{solv}|$ decreases gradually with the structure change of **2**→**3**→**4**, as would be inferred from the discussion of Eq. 3 (vide supra). These results can be understood on the basis of the Born-type equation pertaining to solvation energies, whose generalized form may be written as:[63]

$$E_{solv} = -\frac{1}{2}\left(1-\frac{1}{\varepsilon}\right)\sum_{A,B}\frac{Q_A\cdot Q_B}{R_{AB}} \quad (15)$$

where $\varepsilon$, $Q_A$ and $Q_B$, and $R_{AB}$ indicate a solvent's dielectric constant, the atomic charges on the A and B

atoms, and the atomic distance between A and B respectively. When A=B, $R_{AB}$ stands for atomic radius. If we put $\sum_{A,B}(Q_A \cdot Q_B)/R_{AB} \equiv (Ze)^2/r$ ($r$ is the cavity radius), according to original Born's equation,[64] then the solvation energies on the dianion or dication come out about four times as large as those of the monoanion or monocation. Also, with an increase in the $r$, i. e., with an increase in the molecular size, the solvation energies may decrease. Of course, this tendency is made prominant in doubly charged species than in singly charged ones, as can actually be found in Table 3. In the case of neutral molecules of BAH, the $\pi$-formal charge at each carbon atom is zero in the PPP calculations; their molecular dipole moments are also zero in a good approximation. Our CNDO/2 calculations gave similar results. These circumstances suggest that the solute-solvent interactions and the solvation energies of neutral BAH's turn out to be the same order for any BAH and very small[45] in comparison with those of the ionic species. Thus, we believe that the solvation energies here evaluated are quite close to those of the ion species themselves, although the values are obtained as the difference between the ion species and the neutral species. Finally, we can say that the standard reduction and oxidation potentials of BAH attributable to the formation of mono- and dianions and mono- and dications, and their mutual relations, can both be well-understood by applying the theories of the PPP-type semiempirical molecular orbitals and the Born-type solvation energies. The present quantitative discussion, pertinent to dianions and dications throughout the monoanions and monocations and to their mutual correlations, seems to be the first to treat BAH.

## Appendix

Let us consider Eq. A-1, written as a linear combination of two variables, $x_1$ and $x_2$:

$$y = a_0 + a_1x_1 + a_2x_2 \qquad \text{(A-1)}$$

The condition necessary to satisfy simultaneously both equations, $y=a_0'+a_1x_1$ and $y=a_0''+a_2x_2$, is that the correlation coefficient, $r_{12}$, between $x_1$ and $x_2$ be perfectly zero. However, when the linear relation $y=b_0+b_1x_1$ is experimentally or theoretically assumed, then it can easily be verified that the $x_2$ should fulfill either one of the conditions, that $x_2$ be constant or be in a linear relation to the $y$ values, i. e., $y=b_0'+b_2x_2$. Multiple regression analysis[65] shows, that if the above $r_{12}$ is not zero, the $a_2$ value in Eq. A-1 is equal to the regression coefficient relevant to the single regression equation of $y$ to the "residual," which is obtained by removing the $x_1$ effect from $x_2$. The same situation also holds for the physical meaning of the $a_1$ value in Eq. A-1, so that the $a_1$ and $a_2$ values in Eq. A-1 are theoretically somewhat complex, especially in the case of a large $r_{12}$ value.

The authors wish to express their thanks to Professor Kōsuke Izutsu of the Faculty of Science, Shinshu University, for his encouragement and his helpful discussions on the problem of the mutual relation between reduction and oxidation potentials throughout the first and second steps.

### References

1) Presented at the Symposia on the Structure Chemistry and Electronic State of Molecules (Tokyo, Sept., 1985, Abstract, p. 166) and Polarography and Electroanalytical Chemistry (Tokyo, Nov., 1986, Abstract, p. 1).

2) G. J Hoijtink, J. van Schooten, E. de Boer, and W. Y. Aalbersberg, *Rec. Trav. Chim.*, **73**, 355 (1954); B. I. Shapiro, V. M. Kazakova, and Y. K. Syrkin, *J. Structural Chem. (USSR)*, **6**, 516, 540 (1965).

3) P. H. Given and M. E. Peover, *J. Chem. Soc.*, **1960**, 385.

4) T. Kubota, Y. Ōishi, K. Nishikida, and H. Miyazaki, *Bull. Chem. Soc. Jpn.*, **43**, 1622 (1970).

5) R. F. Michielli and P. J. Elving, *J. Am. Chem. Soc.*, **90**, 1989 (1968).

6) G. J. Hoytink, "Advances in Electrochemistry and Electrochemical Engineering," John Wiley & Sons, New York (1970), Vol. 7, pp. 221—281.

7) A. J. Bard, A. Ledwith, and H. J. Shine, *Adv. Phys. Org. Chem.*, **13**, 155 (1976).

8) V. D. Parker, *Adv. Phys. Org. Chem.*, Academic Press, **19**, 131 (1983).

9) M. E. Peover, "Electroanalytical Chemistry," ed by A. J. Bard, Marcel Dekker, New York (1967), Vol. 2, Chap. 1.

10) Rafik O. Loutfy and Raouf O. Loutfy, *J. Phys. Chem.*, **77**, 336 (1973).

11) Rafik O. Loutfy and Raouf O. Loutfy, *Can. J. Chem.*, **54**, 1454 (1976); Rafic O. Loutfy and Raouf O. Lautfy, *J. Phys. Chem.*, **76**, 1650 (1972).

12) T. Kubota, H. Miyazaki, M. Yamakawa, K. Ezumi, and Y. Yamamoto, *Bull. Chem. Soc. Jpn.*, **52**, 1588 (1979) and the others of our papers cited therein.

13) J. Koutecký, *Z. Phys. Chem. (N. F.)*, **52**, 8 (1967).

14) M. J. S. Dewar, J. A. Hashmall, and N. Trinajstrić, *J. Am. Chem. Soc.*, **92**, 5555 (1970).

15) V. D. Parker, *J. Am. Chem. Soc.*, **98**, 98 (1976).

16) B. Case, N. S. Hush, R. Parsons, and M. E. Peover, *J. Electroanal. Chem.*, **10**, 360 (1965).

17) A. Streitwieser Jr., "Molecular Orbital Theory for Organic Chemists," John Wiley & Sons, New York (1961), p. 173.

18) T. Kubota, K. Nishikida, H. Miyazaki, K. Iwatani, and Y. Ōishi, *J. Am. Chem. Soc.*, **90**, 5080 (1968).

19) B. Uno, Y. Matsuhisa, K. Kano, and T. Kubota, *Chem. Pharm. Bull.*, **32**, 1 (1984), and the other references given therein.

20) N. S. Hush and J. Blackledge, *J. Chem Phys.*, **23**, 514 (1955).

21) S. Hünig, D. Scheutzow, P. Čársky, and R. Zahradnik, *J. Phys. Chem.*, **75**, 335 (1971); P. Čársky, S. Hünig, D. Scheutzow, and R. Zahradnik, *Tetrahedron*, **25**, 4781 (1969).

22) M. Senda and R. Takahashi, *Rev. Polarogr. (Kyoto)*, **20**, 56 (1974).

23) T. Kakutani, Y. Morihiro, M. Senda, R. Takahashi, and K. Matsumoto, *Bull. Chem. Soc. Jpn.*, **51**, 2847 (1978).

24) O. Hammerich and V. D. Parker, *Electrochim. Acta*, **18**, 537 (1973).

25) K. Kano, T. Konse, N. Nishimura, and T. Kubota, *Bull. Chem. Soc. Jpn.*, **57**, 2383 (1984).

26) T. Kubota, B. Uno, Y. Matsuhisa, H. Miyazaki, and K. Kano, *Chem. Pharm. Bull.*, **31**, 373 (1983).

27) In the case of reduction-CV measurements, a Metrohm EA 290 hanging-mercury-drop electrode was also used, but the reduction potentials concurred within a several mV with those obtained using the Pt electrode for all the samples employed. All the discussion in this text was, therfore, carried out using the data obtained by the use of the Pt electrode.

28) T. Kubota, H. Miyazaki, K. Ezumi, and M. Yamakawa, *Bull. Chem. Soc. Jpn.*, **47**, 491 (1974).

29) J. Juillard, "Recommended Methods for Purification of Solvents and Tests for Impurities," ed by J. F. Coetzee, (IUPAC), Pergamon Press, Oxford (1982), p. 32; J. F. Coetzee, *ibid.* (1982), p. 1.

30) The Merck Index was referred to in choosing the solvents. "The Merck Index," 9th, ed., ed by M. Windholz, S. Budavari, L. Y. Stroumtsos, and M. N. Fertig, Merck & Co., New Jersey (1976).

31) That the dianion of BAH may exist in either a singlet or triplet state is well known.[32] The present calculation was performed for the singlet closed system, since, if LUMO does not degenerate, the singlet species is usually more stable than in the triplet state, though the energy difference is not very large for common BAH dianions.

32) A. Minsky, A. Y. Meyer, R. Poupko, and M. Rabinovitz, *J. Am. Chem. Soc.*, **105**, 2164 (1983).

33) The ground state of LP-SCFMO calculation is not completely in the so-called SCF state,[34] so excited configurations are slightly mixed in the ground state. Neglecting this effect, the MO's were employed in this discussion.

34) H. C. Longuet-Higgins and J. A. Pople, *Proc. Phys. Soc. London Sec. A*, **68**, 591 (1955); A. Ishitani and S. Nagakura, *Theor. Chim. Acta (Berlin)*, **4**, 236 (1966); R. Zahradnik and P. Čársky, *J. Phys. Chem.*, **74**, 1235, 1240, 1249 (1970); K. Ezumi, T. Kubota, H. Miyazaki, and M. Yamakawa, *J. Phys. Chem.*, **80**, 980 (1976).

35) K. Nishimoto and L. S. Forster, *Theor. Chim. Acta (Berlin)*, **4**, 155 (1966).

36) Although the molecular dimensions seem to be somewhat different among the neutral, monoanion and monocation, and dianion and dication species, this was neglected since the effect seems to be small for the present rigid molecule.

37) N. Mataga and K. Nishimoto, *Z. Physik. Chem. (N. F.)*, **13**, 140 (1957).

38) Here, $E_{solv}$, $E^{-}_{solv}$, and $E^{=}_{solv}$ are the solvation energies for the neutral molecule, the monoanion radical, and the dianion respectively.

39) T. Koopmans, *Physica*, **1**, 104 (1933).

40) B. S. Jensen and V. D. Parker, *J. Am. Chem. Soc.*, **97**, 5211 (1975).

41) A rather large difference is found in the $E^{red}_{1/2\cdot2}$ value of **7** (chrysene), −2.730 V having been reported by Jensen and Parker.[40]

42) Also, we would expect a linear $E^{red}_{1/2\cdot1}$ vs. $E_A$ (electron affinity) relation for the present BAH series, since $E_A$ is parallel with $\varepsilon_{lu}$. The results are $E^{red}_{1/2\cdot1}=1.154E_A-2.759$, with $r=0.946$ and $n=6$ (Compounds **1**, **2**, **5**—**7**, **10**), the $E_A$ values being cited from Ref. 43 and given in Table 2.

43) W. E. Wentworth, E. Chen, and J. E. Lovelock, *J. Phys. Chem.*, **70**, 445 (1966).

44) As may be understood from Fig. 2, if we choose such polyacenes as Compounds **2**—**4**, the $E^{red}_{1/2\cdot2}$ vs. $\varepsilon^{=}_{ho}$ plot of Eq. 3 gives a very good linear correlation. This kind of result was also found on the other plottings. The topological MO and molecular features of polyacenes may play an important role in this result.

45) N. Mataga and T. Kubota, "Molecular Interactions and Electronic Spectra," Marcel Dekker, New York (1970).

46) A. Carrington and A. D. McLachlan, "Introduction to Magnetic Resonance," Harper & Row, New York and London (1967).

47) Also, the Boltzmann distribution equilibrium between singlet and triplet states has been pointed out for the ground states of BAH dianions;[32] this fact may somewhat complicate the nature of the dianion in solution.

48) R. O. Loutfy, *J. Chem. Phys.*, **66**, 4781 (1977).

49) That the two-electron-repulsion-integrals ($\gamma_{ll}$, $\gamma^{-}_{ss}$, $\gamma^{+}_{ss}$) will have quite a large molecular-size dependence can easily be understood from, for example, the electron's angular correlation effect.[50].

50) C. Sandorfy, "Electronic Spectra and Quantum Chemistry," Prentice-Hall, New Jersey (1964).

51) R. J. Klingler and J. K. Kochi, *J. Am. Chem. Soc.*, **102**, 4790 (1980); J. O. Howell, J. M. Goncalves, C. Amatore, L. Klasinc, L. R. M. Wightman, and J. K. Kochi, *ibid.*, **106**, 3968 (1984).

52) R. Boschi, E. Clar, and W. Schmidt, *J. Chem Phys.*, **60**, 4406 (1974).

53) Dewar et al. reported this equation;[14] $E^{oxd}_{1/2\cdot1}=0.996I^{cal}_{P}-6.607$, with $r=0.987$ and $n=9$, and where $I^{cal}_{P}$ is the $I_P$ calculated by them.

54) It is well known that the dications of 9,10-dimethyl- (see Table 2) and 9,10-diphenylanthracenes[24] are cyclic voltammetrically stable.

55) a) A. D. McLachlan, *Mol. Phys.*, **4**, 49 (1961). b) A. D. McLachlan, *Mol. Phys.*, **2**, 271 (1959). c) T. Shida and S. Iwata, *J. Am. Chem. Soc.*, **95**, 3473 (1973).

56) In the case of the $E^{red}_{1/2\cdot1}$ and $E^{red}_{1/2\cdot2}$ measurements, DMF and AN gave almost the same values for perylene when a Pt electrode was used (see Table 2). This fact is reasonable judging from the Born equation, because the dielectric constants[29] of DMF (37.0) and AN (36.0) are almost equal to each other.

57) N. S. Hush and A. J. Pople, *Trans. Faraday Soc.*, **59**, 600 (1955); R. M. Hedges and F. A. Matsen, *J. Chem. Phys.*, **28**, 950 (1958); R. S. Becker and W. E. Wentworth, *J. Am. Chem. Soc.*, **85**, 2210 (1963); J. R. Hoyland and L. Goodman, *J. Chem. Phys.*, **36**, 21 (1962).

58) R. S. Mulliken, *J. Chem. Phys.*, **2**, 782 (1934); **3**, 537 (1935).

59) a) This relation was employed by Senda and Takahashi[22,23] to determine the standard electrode potential in nonaqueous solvents. b) Our data in Table 2 were obtained in DMF for reduction, but in AN for oxidation; thus, we can not omit the error due to the solvation-energy difference brought about by DMF and AN, though the difference is quite small.[56] Parker[15] reported the values of

$(E^{oxd}_{1/2\cdot1}+E^{red}_{1/2\cdot1})/2$ for BAH in AN; they are $-0.313\pm0.022$ V ($n$=10) and $\Delta E^{+}_{solv}=\Delta E^{-}_{solv}$ within the limits of experiment error, though they adopted irreversible CV data for $E^{oxd}_{1/2\cdot1}$.

60) The coefficient of $\varepsilon_{lu}$ or $\varepsilon_{ho}$ in Eqs. 1 and 2 is constrained to unity on the assumption that, if the MO evaluation of the energies is correct, the coefficient becomes 1.

61) Parker[15] reported $\Delta G°=-4.4$ eV vs. SCE on the basis of the same treatment as was used here. Peover et. al.[16] reported $\Delta G°=-4.70$ eV in the case of the ($Ag/Ag^{+}$) electrode in AN. Alternatively, $\Delta G°$ values of $-4.36$ to $-4.41$ eV have also been reported for SCE.[62]

62) R. C. Larson, R. T. Iwamoto, and R. N. Adams, *Anal. Chim. Acta*, **25**, 371 (1961); J. E. Kuder, D. Wychick, R. L. Miller, and M. S. Walker, *J. Phys. Chem.*, **78**, 1714 (1974).

63) I. Jano, *C. R. Acad. Sci. (Paris)*, **261**, 103 (1963); O. Kikuchi, T. Kozaki, and K. Morihashi, *Nippon Kagaku Kaishi*, **1986**, 1409.

64) M. Born, *Z. Phys*, **1**, 45 (1920).

65) T. Okuno, H. Kume, T. Haga, and T. Yoshizawa, "Multivariate Analysis," (in Japanese), Nikkagiren Press, Tokyo (1978), Chapter II; N. R. Draper and H. Smith, "Applied Regression Analysis," John Wiley & Sons, New York (1968).